

CHEMISTRY & SUSTAINABILITY

CHEM **SUS** CHEM

ENERGY & MATERIALS

Accepted Article

Title: Selective Hydrodeoxygenation of 5-Hydroxymethylfurfural to 2,5-Dimethylfuran over Heterogeneous Iron Catalysts

Authors: Jiang Li, Jun ling Liu, He Yang Liu, Guang yue Xu, Jun jie Zhang, Jia xing Liu, Guang lin Zhou, Qin Li, Zhi hao Xu, and Yao Fu

This manuscript has been accepted after peer review and appears as an Accepted Article online prior to editing, proofing, and formal publication of the final Version of Record (VoR). This work is currently citable by using the Digital Object Identifier (DOI) given below. The VoR will be published online in Early View as soon as possible and may be different to this Accepted Article as a result of editing. Readers should obtain the VoR from the journal website shown below when it is published to ensure accuracy of information. The authors are responsible for the content of this Accepted Article.

To be cited as: *ChemSusChem* 10.1002/cssc.201700105

Link to VoR: <http://dx.doi.org/10.1002/cssc.201700105>

WILEY-VCH

www.chemsuschem.org

A Journal of



Selective Hydrodeoxygenation of 5-Hydroxymethylfurfural to 2,5-Dimethylfuran over Heterogeneous Iron Catalysts

Jiang Li,^[a] Jun-ling Liu,^[a] He-yang Liu,^[a] Guang-yue Xu,^[b] Jun-jie Zhang,^[a] Jia-xing Liu,^[a] Guang-lin Zhou,^[a] Qin Li,^[a] Zhi-hao Xu,^[a] and Yao Fu^{*,[b]}

Abstract: This work provided the first example of selective hydrodeoxygenation of 5-hydroxymethylfurfural to 2,5-dimethylfuran over heterogeneous iron catalysts. Catalyst prepared by the pyrolysis of iron-phenanthroline complex on activated carbon at 800 °C was demonstrated to be the most active heterogeneous iron catalyst. Under the optimal reaction condition, complete conversion of HMF was achieved with an 86.2% selectivity of DMF. The reaction pathway was investigated thoroughly, and the hydrogenation of C=O bond in HMF was demonstrated to be the rate-determining step during the hydrodeoxygenation, which will be accelerated greatly by using alcohol solvents as additional H-donors. The excellent stability of the iron catalyst was demonstrated in batch and continuous flow fixed-bed reactors, which was probably due to the well reserved active species and the pore structure of the iron catalyst in the presence of H₂.

Introduction

The utilization of renewable sources especially lignocellulosic biomass to replace fossil reserves to produce fuel and chemicals has recently attracted significant attention.^[1,2] 5-Hydroxymethylfurfural (HMF), which can be produced from biomass-derived hexoses through acidic hydrolysis, has been considered as one of the most important platform chemicals during biomass conversion.^[3] The high functionality of HMF allows it to be converted to various biofuel molecules such as ethyl levulinate,^[4] 5-ethoxymethylfurfural,^[5] 2,5-dimethylfuran,^[6] and value-added chemicals such as levulinic acid,^[7] furfuryl alcohol,^[8] 2,5-diformylfuran,^[9] 2,5-furandicarboxylic acid,^[10] terephthalic acid,^[11] and caprolactone.^[12] Among these HMF derivatives, 2,5-dimethylfuran (DMF) is particularly attractive. It was proposed as a more promising transportation fuel due to its higher energy density, higher boiling point and lower solubility in water as compared to ethanol.

The first example of the generation of DMF from biomass-derived carbohydrates was reported by Dumesic et al.^[6] The whole process was achieved by selective dehydration of fructose to HMF in a biphasic system followed by the hydrodeoxygenation (HDO) of HMF to DMF over a chloride-resistant carbon-supported copper-ruthenium (CuRu/C) catalyst. The yield of DMF from HMF was 76~79%. Inspired by their work various researches aimed at developing more efficient catalyst systems for the HDO of HMF to DMF were carried out, and most of them are based on noble metals such as Pd, Ru and Pt. Rauchfuss et al. reported that the combination of Pd/C catalyst and formic acid solvent enables an efficient one-pot synthesis of DMF from fructose with a total yield of 51%.^[13] Meanwhile, Bell et al. reported a two-step process involving heteropoly acids catalyzed dehydration of glucose to HMF and subsequent HDO of HMF with Pd/C catalyst in ionic liquids with the addition of acetonitrile.^[14] Saha et al. reported a one-pot conversion of lignocellulosic and algal biomass into DMF by using a multicomponent catalytic system consisted of [DMA]⁺[CH₃SO₃]⁻, Ru/C, and formic acid.^[15] Vlachos et al. reported the catalytic transfer hydrogenation (CTH) of HMF to DMF using secondary alcohols as the hydrogen donors over a Ru/C catalyst with a DMF yield of up to 80%.^[16] and then the role of Ru and RuO₂ phases was studied in detail.^[17] Hermans et al. reported the CTH of HMF to DMF over Fe₂O₃-supported Pd catalyst with 2-propanol as hydrogen donor, and the yield of DMF was 72%.^[18] Wang et al. reported the HDO of HMF over a Ru/Co₃O₄ catalyst at 130 °C and 0.7 MPa H₂ in Tetrahydrofuran (THF), and the yield of DMF was 93.4%.^[19] Hu et al. studied the HDO of HMF over a Ru/C catalyst in THF at 200 °C for 2 h, and 94.7% DMF yield with 100% HMF conversion was achieved.^[20] Kawanami et al. reported the use of supercritical carbon dioxide–water on the HDO of HMF over a Pd/C catalyst, and a very high yield (100%) of DMF was observed at 80 °C for 2 hours.^[21] More recently, the HDO of HMF to DMF over Ru/NaY, Ru/HT, Pt/C, Pt/rGO, and Pd-Cs_{2.5}H_{0.5}PW₁₂O₄₀/K-10 clay catalysts have also been reported.^[22-26]

Besides above-mentioned monometallic catalyst systems, the HDO of HMF to DMF over noble metal-based bimetallic catalysts has also been reported. Notably, Schuth et al. reported that PtCo bimetallic nanoparticles could be used as highly efficient catalyst for the HDO of HMF to DMF in butanol.^[27] The conversion of HMF achieved 100% within 10 min, and the yield of DMF reached 98% after 2 h. Subsequently, Gorte et al. further explored the mechanism for this high selectivity.^[28] The formation of a monolayer oxide on the surface of the metallic core was suggested as the fundamental principle, which interacts weakly with the furan ring to prevent overhydrogenation and ring opening of DMF while providing active sites for the HDO reaction. In addition, Pt-Ni, Pt-Zn and Pt-Cu alloyed nanocrystals have also been demonstrated to be effective catalysts for HMF HDO with 98% DMF yield.^[29] Dumesic et al. reported that DMF can be produced with 46%

- [a] Dr. J. Li, J.-L. Liu, H.-Y. Liu, J.-J. Zhang, J.-X. Liu, Dr. G.-L. Zhou, Q. Li, Z.-H. Xu
State Key Laboratory of Heavy Oil Processing
Institute of New Energy
China University of Petroleum (Beijing)
Beijing 102249, China
Fax: (+86) 010-89731300
Email: lijia@cup.edu.cn
- [b] G.-Y. Xu, Prof. Dr. Y. Fu
Anhui Province Key Laboratory of Biomass Clean Energy
Department of Chemistry
University of Science and Technology of China
Hefei 230026, China
Fax: (+86) 551-3606689
E-mail: fuyao@ustc.edu.cn

Supporting information for this article is given via a link at the end of the document.

yield by hydrogenolysis of HMF in the presence of lactones using a RuSn/C catalyst at 200 °C.^[30] Abu-Omar et al. reported that a bimetallic catalyst which contained a Lewis-acidic Zn^{II} and Pd/C components was effective for the HDO of HMF to DMF with high conversion (99%) and selectivity (85%).^[31] Ebitani et al. reported a bimetallic Pd₅₀Au₅₀/C catalyst catalyzed HDO of HMF to DMF in the presence of hydrochloric acid (HCl) under an atmospheric hydrogen pressure.^[32]

Considering the high cost and scarcity of noble metals, the HDO of HMF to DMF over non-noble metal catalysts was investigated recently. The activities and stabilities of six carbon-supported noble or non-noble metal catalysts had been compared in a continuous flow reactor by Gorte et al.^[33] Barta et al. reported the catalytic conversion of HMF over a Cu-doped porous metal oxide in supercritical methanol, and a combined yield (DMF + DMTHF) of 58% was achieved.^[34] Subsequently, they studied the conversion of HMF over Cu_{0.61}Mg_{2.33}Al_{0.98}Ru_{0.02} and copper–zinc nanoalloy catalysts, and up to 97% combined products yields were obtained at 200–220 °C using 20–30 bar H₂.^[35,36] Fu et al. used nickel–tungsten carbide and perovskite type oxide supported Ni catalysts for the conversion of HMF into DMF.^[37,38] Zhu et al. reported a series of researches concerning about the catalytic conversion of HMF over non-noble metal catalysts such as Raney Ni, NiSi-PS, Ni/Al₂O₃ and mineral-derived Cu catalysts.^[39–42] They also studied the one-step continuous conversion of fructose to DMF over combined HY zeolite and hydrotalcite (HT)-Cu/ZnO/Al₂O₃ in a fixed-bed reactor with a DMF yield of 40.6%.^[43] Wang et al. studied the catalytic transfer hydrogenation/hydrogenolysis of HMF to DMF over a carbon supported nickel-cobalt catalyst with formic acid as hydrogen donor with the highest DMF yield of 90.0%.^[44] Yuan et al. recently reported that Cu-Co bimetallic nanoparticles coated with carbon layers were very efficient catalyst for the HDO of HMF to DMF.^[45] The key issue for these Cu and Ni-based promising catalyst system is how to suppress the overhydrogenation of the aromatic furan ring and the ring-opening of DMF to improve the selectivity of DMF.

Iron is an abundant, eco-friendly, relatively nontoxic, and inexpensive element, and thus, a very promising alternative to precious metals in catalysis. However, to the best of our knowledge, the possibility of iron-catalyzed HMF HDO to DMF was still questionable. For example, a DMF yield of 91.3% could be achieved over carbon nanotube-supported bimetallic Ni-Fe (Ni-Fe/CNT) catalysts, but trace yield of DMF was obtained over Fe/CNT catalyst with only 3.2% conversion of HMF.^[46]

Recently, nitrogen-doped carbon materials supported iron catalysts has attracted much attention in some important chemical reactions such as oxygen reduction reaction (ORR) and nitroarenes hydrogenation.^[47–49] Beller et al. reported some pioneer works using heterogeneous iron catalysts for organic synthesis, for example selective hydrogenation of nitroarenes, green synthesis of nitriles and green reductive aminations.^[49–51] Inspired by their works, we recently reported the efficient CTH of furfural to furfuryl alcohol over heterogeneous iron catalysts.^[52] In this work, the first example of iron-catalyzed HDO of HMF to DMF was reported. Under the optimal reaction condition, complete conversion of HMF was achieved with an 86.2%

selectivity of DMF. The detail study of the reaction pathway indicated that the hydrogenation of C=O bond was the rate-determining step, which will be boosted greatly by using alcohols as both solvents and additional H-donors. The excellent stability of iron catalysts was proved in batch and continuous flow fixed-bed reactors. Thus, nitrogen-doped activated carbon-supported iron catalysts were demonstrated to be an effective, stable catalyst system for the HDO of HMF to DMF.

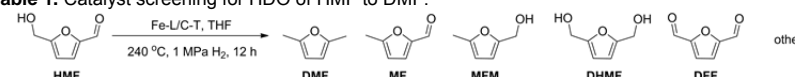
Results and Discussion

Catalyst screening

The fabrication process for the iron catalysts was the same as our previous study, which was generally involved the simultaneous pyrolysis of metal precursors and nitrogen precursors on several supports at a pyrolysis temperature ranged from 400 °C to 1000 °C (see figure S1 in the supporting information).^[52] Five compounds are used as nitrogen precursors including 1,10-phenanthroline (L1), 2,2'-bipyridine (L2), 2,2';6',2"-terpyridine (L3), 8-hydroxyquinoline (L4) and phenylglycine (L5). A native iron complex, hemin (6) was directly used as the precursor of metal and nitrogen. Activated carbon, SiO₂, and Al₂O₃ were used as the supports. The as-prepared catalysts were denoted as Fe-Ln/S-T, where Ln represents the type of nitrogen precursor, S represents the type of support, and T represents the pyrolysis temperature. The catalyst prepared from hemin was denoted as 6/C-800.

The HDO of HMF to DMF over heterogeneous iron catalysts was first investigated at 240 °C 1MPa H₂ in THF, which has been demonstrated to be a good solvent for heterogeneous iron catalysis and HMF conversion.^[37,49] A glass vial was used to exclude the influence of reactor body. Besides the target product DMF, 5-methylfurfural (MF), 5-methyl-2-furanmethanol (MFM), 2,5-dihydroxymethylfuran (DHMF), and 2,5-diformylfuran (DFF) were also observed as by-products. In addition, the absence of ring-hydrogenated products such as 2,5-dimethyl tetrahydrofuran (DMTHF), 2-hexanone, and tetrahydrofurfural alcohol demonstrated that the iron catalysts did not hydrogenate the aromatic rings of furanic compounds. The carbon mass balance(CMB) was calculated based on the detected known products.

In the blank test, only 1.1% yield of DMF was observed (Table 1, entry 1), indicating that the HDO of HMF to DMF was unlikely to occur without any catalysts. In addition, 11.3% yield of MF indicated the occurrence of C-O bond HDO. The yield of DMF increased significantly in the presence of heterogeneous iron catalysts. Catalysts prepared from different nitrogen precursors were investigated at first (entry 2-7). Fe-L1/C-800 catalyst gave a highest DMF yield of 32.5%, and MF and DFF were observed as major by-products with yields of 30.3% and 7.5%, respectively. The generation of DFF during HMF HDO, which was further demonstrated by the GCMS spectrum (figure S2A), has rarely been reported before. While the iron-catalyzed CTH was confirmed in a later section, we proposed that DFF was

Table 1. Catalyst screening for HDO of HMF to DMF.^[a]


Entry	Catalysts	Conversion [%]	Yield [%]					CMB ^[b] [%]
			DMF	MF	MFM	DHMF	DFF	
1	-	19.6	1.1	11.3	0.4	0.2	-	13.0
2	Fe-L1/C-800	73.0	32.5	30.3	0.1	0.5	7.5	70.9
3	Fe-L2/C-800	34.4	6.6	23.7	<0.1	0.1	0.8	31.2
4	Fe-L3/C-800	55.0	15.8	26.6	0.2	0.6	7.3	50.5
5	Fe-L4/C-800	35.3	3.9	15.2	<0.1	0.1	10.0	29.2
6	Fe-L5/C-800	41.9	14.9	12.9	<0.1	0.1	10.3	38.2
7	6/C-800	70.7	30.7	30.8	0.3	0.3	1.1	63.2
8	Fe-L1/SiO ₂ -800	67.8	11.4	45.1	0.1	0.5	6.3	63.4
9	Fe-L1/Al ₂ O ₃ -800	35.7	14.1	11.7	0.4	0.2	0.4	26.8
10	Fe-L1/TiO ₂ -800	44.3	9.8	19.1	4.1	1.4	5.3	39.7
11	Fe-L1/C-400	70.4	5.0	20.3	0.5	0.2	16.4	42.4
12	Fe-L1/C-600	74.9	12.5	30.5	0.6	0.1	4.3	48.0
13	Fe-L1/C-1000	34.5	5.2	13.3	<0.1	0.9	5.5	24.9
14	Fe/C-800	29.2	10.4	5.8	0.3	0.2	3.4	20.1
15	L1/C-800	45.6	8.9	20.5	<0.1	0.2	5.8	35.4
16	Fe-L1	17.0	0.5	8.4	0.9	0.9	3.9	14.6
17	Fe	28.9	4.2	8.7	0.2	0.2	4.5	17.8
18	L1	30.1	1.8	19.8	1.3	0.5	0.8	24.2
19	C	23.4	1.2	6.9	-	-	6.9	15.0
20	Co-L1/C-800	96.8	41.5	23.6	0.3	0.9	6.4	72.7
21	Ni-L1/C-800	52.2	24.6	24.3	0.2	0.1	0.3	49.5

[a] Reaction conditions: 0.5 mmol HMF, 20 mL THF, 0.1 g iron catalyst, 1 MPa H₂, t=12h. The molar ratio of iron/HMF was kept at 11.2 mol%. [b] CMB is carbon mass balance, which is calculated based on the detected known products.

generated by the dehydrogenation of HMF when HMF itself acted as H-donor during the reaction. Catalyst prepared from native iron complex (6/C-800) gave a slightly lower DMF yield of 30.7%. In contrast, catalysts prepared from L2-L5 gave much lower DMF yields. Thus, 1,10-phenanthroline (L1) was the most effective nitrogen precursor.

Besides using activated carbon as the support, some metal oxides such as SiO₂, Al₂O₃, and TiO₂ were also examined (entry 8-10). Much lower yields of DMF were obtained, confirming that activated carbon was the most effective support. Subsequently, the effect of pyrolysis temperature was also investigated (entry 11-13). The decrease of pyrolysis temperature from 800 °C to 600 or 400 °C leads to a sharp decrease in DMF yield. In addition, when the pyrolysis temperature was further raised to 1000 °C, significant decrease in both HMF conversion and DMF yield were also observed. These results confirmed that the optimal pyrolysis temperature was 800 °C.

Catalysts prepared by the pyrolysis of iron precursor or nitrogen precursor on carbon support exhibited an inferior catalytic activity towards the HDO of HMF (entry 14, 15). In addition, the direct use of iron complex (Fe-L1), iron acetate (Fe), 1,10-phenanthroline (L1), or carbon support (C) also exhibited poor catalytic performances (entry 16-19). Thus, the simultaneous pyrolysis of iron precursor and nitrogen precursor on carbon support was critical to its catalytic activity.

The replacement of the metal center iron with cobalt led to enhanced HMF conversion and DMF yield. However, the yield of unidentified products also increased to 24.1%. This cobalt-catalyzed HMF HDO will be studied in detail in our further works. In addition, when the metal center was replaced by nickel, a decrease in the catalytic performance was observed. Although

nickel catalysts have been previously reported to be more effective than iron catalysts in the HDO of furanic compounds,^[53] the pyrolysis of metal-phenanthroline complexes on activated carbon seemed to generate more active iron catalysts than nickel catalysts.^[54]

In our previous research, we have demonstrated that the catalytic activities of the iron catalysts were determined by the nitrogen content and the percentage of N-Fe specie by using various technologies especially XPS characterization.^[52] Moreover, a recent study by Beller et al. demonstrated that the active site in this kind of pyrolyzed iron catalyst was consisted of a unique structure, where iron oxides were surrounded by nitrogen-doped-graphene shells then immobilized on carbon support.^[55] We explored the morphologies of Fe-L1/C-800, Fe-L1/C-400, and Fe-L4/C-800 catalysts by TEM and Energy dispersive X-ray (EDX) analysis (figure S3). No obvious iron particles could be observed in the TEM image of Fe-L1/C-800 catalyst at different

areas, and EDX analysis showed extremely weak signals of iron species. This suggested a homogeneous distribution of iron species on the catalyst surface. In contrast, cloudy agglomerates can be observed in the TEM images of Fe-L1/C-400 and Fe-L4/C-800 catalysts, and stronger signals of iron species can be detected by EDX analysis.

To further explore the Fe configuration, H₂-TPR analysis was performed. It is well known that the Fe₂O₃ species in iron catalysts have two characteristic peaks in the H₂-TPR analysis.^[53] The first broad peak ranging from 410 to 570 °C could be ascribed to the reduction of α-Fe₂O₃ into α-Fe₃O₄. The second broad peak ranging from 590 to 730 °C is typically attributed to the reduction of iron oxides to α-Fe. As shown in figure 1, the characteristic peaks of the Fe₂O₃ species could be clearly observed in the Fe/C-800 catalyst, demonstrating that the Fe₂O₃ species could be formed by the direct pyrolysis of iron acetate onto activated carbon. In addition, we did not observe any diffraction peaks of the Fe₂O₃ phase in the XRD pattern of the Fe/C-800 catalyst,^[52] suggesting that amorphous Fe₂O₃ phase could also be detected by the H₂-TPR analysis. When nitrogen precursors were added into the pyrolysis process, the characteristic peaks of the Fe₂O₃ species could only be found in the Fe-L3/C-800 and Fe-L4/C-800 catalysts. In contrast, only one broad peak ranging from 200 to 800 °C was observed in the H₂-TPR results of the most active Fe-L1/C-800 and 6/C-800 catalysts, and it started from 500 °C and 300 °C for the Fe-L2/C-800 and Fe-L5/C-800 catalysts, respectively. The curve fitting results for the H₂-TPR analysis of Fe-L1/C-800 catalyst suggested that there should be an intense peak at 620 °C besides peaks of Fe₂O₃ species. We proposed that this peak

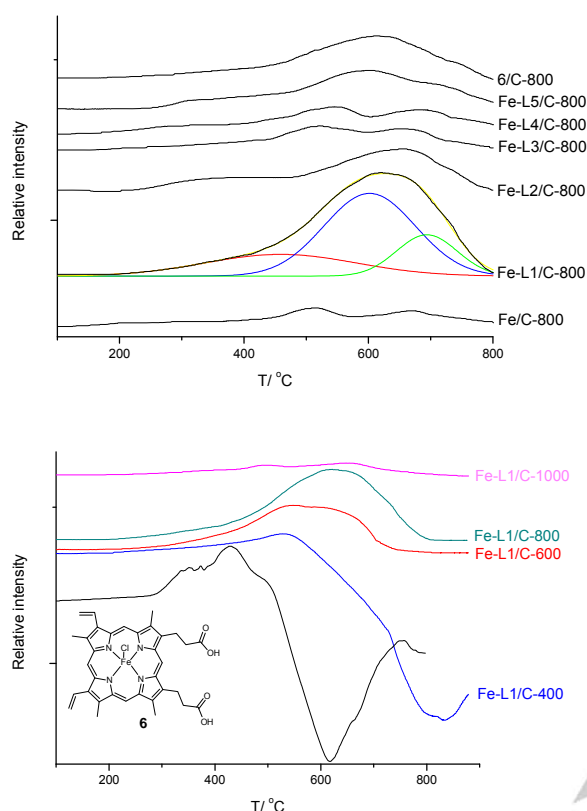


Figure 1. H₂-TPR of various iron catalysts.

could be attributed to the reduction of iron cations coordinated by pyridinic nitrogen functionalities (FeN_x species) to metallic iron. This is hard to be confirmed because of the lack of previous studies about the H₂-TPR analysis of Fe-N-C catalysts to our knowledge.

To test our hypothesis, we tried to explore the H₂-TPR of hemin (previously denoted as 6), which was a native iron complex contained FeN₄ species, and Fe-L1/C catalysts prepared at different pyrolysis temperatures. For hemin, the reduction peak started from 250 °C, which was generally consistent with Fe-L1/C-800 catalyst. Unfortunately, this compound was unstable during H₂-TPR. Some gases were released, leading to a large desorption peak after 500 °C. Thus, the H₂-TPR result of hemin could not directly help us justify previous peak at 620 °C. The desorption peak could also be observed in the H₂-TPR analysis of the Fe-L1/C-400 catalyst, but it achieved

the maximum at a higher temperature around 800 °C. The desorption peak disappeared when the pyrolysis temperature exceeded 600 °C, and only a broad peak could be observed in the H₂-TPR analysis results of the Fe-L1/C-600 and Fe-L1/C-800 catalysts. When the pyrolysis temperature was further increased to 1000 °C, the characteristic peaks of the Fe₂O₃ species at 490 °C and 650 °C could be observed in the H₂-TPR result (see figure S4 for clearer observations). The changes in the H₂-TPR results were consistent with some previous findings, for example the structure of iron oxides surrounded by nitrogen-doped-graphene shells was formed at pyrolysis temperature over 400 °C,^[49] and the active sites of FeN_x species would be decomposed to Fe₂O₃ at a pyrolysis temperature of 1000 °C.^[52] Thus, the peak at 620 °C in the H₂-TPR results is likely the characteristic peak of FeN_x species, which were considered to govern the unique catalytic activity of the iron catalysts in some previous studies.^[49]

Solvent effect

The unsatisfactory catalytic performance of Fe-L1/C-800 catalyst in THF (aprotic polar solvent) required the further optimization of the reaction parameters. Some previous studies indicated that the chemical nature of the solvent have a significant impact on the HDO of HMF to DMF.^[23,35] We further examined the solvent effect in the iron-catalyzed HDO reaction (table 2). When hexane (non-polar solvent) was used as the solvent, HMF conversion and DMF yield was improved slightly, but still far from satisfying. Considering that we have recently reported the efficient catalytic transfer hydrogenation of C=O bond in furfural over iron catalysts by using alcohols as H-donors, it was speculated that the hydrogenation of C=O bond in HMF maybe

Table 2. Catalytic HDO of HMF to DMF over Fe-L1/C-800 catalyst in different solvents.^[a]

Entry	Solvent	Atmosphere	Conversion [%]	Yield[%]					CMB ^[b] [%]
				DMF	MF	MFM	DHMF	DFF	
1	THF	1 MPa H ₂	73	32.5	30.3	0.1	0.5	7.5	70.9
2	Hexane	1 MPa H ₂	100	45.5	5.1	-	-	2.5	53.1
3	MeOH	1 MPa H ₂	100	42.1	7.2	0.2	<0.1	1.1	50.6
		Without H ₂	100	15.0	5.4	9.3	-	0.1	29.8
4	EtOH	1 MPa H ₂	100	64.1	1.4	<0.1	-	-	65.5
		Without H ₂	100	54.1	0.2	-	-	-	54.3
5	1-PrOH	1 MPa H ₂	100	69.1	0.5	0.4	0.1	0.5	70.6
		Without H ₂	100	50.3	-	-	-	-	50.3
6	2-PrOH	1 MPa H ₂	100	60.8	-	-	-	-	60.8
		Without H ₂	100	52.1	0.3	-	-	-	52.4
7	1-BuOH	1 MPa H ₂	100	75.3	0.6	-	0.5	-	76.4
		Without H ₂	100	67.4	-	-	-	-	67.4
8	2-BuOH	1 MPa H ₂	99.7	60.9	0.1	0.2	0.2	-	61.4
		Without H ₂	100	55.3	-	-	-	-	55.3

[a] Reaction conditions: 0.5 mmol HMF, 20 mL solvent, 0.1 g Fe-L1/C-800 catalyst, t=12h. [b] CMB is carbon mass balance, which is based on the detected known products.

could also be boosted by using alcohols as the solvent. Thus, various primary and secondary alcohols were used to investigate the solvent effect (Table 2, entry 3-8). It can be clearly seen that the yield of DMF was increased dramatically with a significant drop in the yield of MF, confirming that there was a substantial enhancement in the hydrogenation of C=O bond. Moreover, we still do not observe any ring-hydrogenated products, indicating that using alcohols as the solvent will not promote the hydrogenation of the furan ring. However, an unsatisfactory carbon mass balance was observed during the reaction. The polymerization of HMF to humins was probably the main reason for the low carbon balance, which will be discussed later in the reaction pathways section.

To further check the role of the alcohols, reactions were also performed in an inert atmosphere (0.5 MPa N_2). While using methanol as the solvent, a significant drop in DMF yield was observed in the absence of H_2 . By comparison, only slight decreases in DMF yields were observed while using alcohols with a carbon number of >2 . Thus, it is concluded that the alcohols with medium chain lengths will act as H-donors in the HDO of HMF and provide alternative hydrogen source besides gaseous hydrogen. The GCMS spectrum strongly confirmed that the CTH reaction occurred even at a H_2 pressure of 4 MPa. Large amount of butyraldehyde dibutyl acetal (see figure S2B, RT=18.088 min) could be observed when n-butanol was used as the solvent at 4 MPa H_2 . It is the aldol condensation product formed from n-butanol and butyraldehyde (the dehydrogenation product of n-butanol produced in the CTH process). The molar ratio of butyraldehyde dibutyl acetal to DMF was 0.23 at 0.5 h, and then increased to 0.6-0.7 after 3 h. In comparison, the molar ratio of butyraldehyde dibutyl acetal to DMF was 2.2 when the reaction was performed under inert atmosphere. Thus, it could be concluded that both the H-donor and gaseous H_2 supplied the hydrogen consumed during the HDO of HMF to DMF.

The yield of DMF increased along with the increase in alcohol chain length from methanol to n-butanol, which is probably due to the dehydrogenation activity of the alcohol (Table S1, see the supporting information). In addition, reactions performed in primary alcohols gave slightly higher DMF yields than in secondary alcohols, although secondary alcohols represented higher dehydrogenation activity than primary alcohols. This solvent effect was probably attributed to solubility of hydrogen, thermal interaction between HMF and the solvent molecules, and competitive adsorption onto the catalytic sites,^[56] which was still needed to confirm in future works.

Effect of reaction temperature and H_2 pressure

The effect of reaction temperature was investigated from 120 to 280 °C at 1 MPa with the Fe-L1/C-800 catalyst, and the results were shown in figure 2. Accordingly, it was found that the reaction temperature played an important role in the HDO of HMF. The absence of DMF with low yields of intermediates such as MFM, MF and DHMF indicated that the HDO of HMF to DMF was unlikely to occur at 120 °C. When the reaction temperature was increased to 160 °C, the DMF yield increased slightly with a

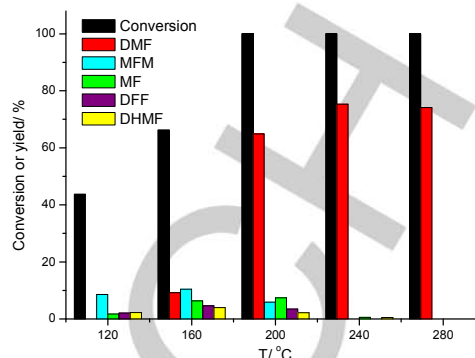


Figure 2. Effect of reaction temperature on the HDO of HMF to DMF. Reaction conditions: 0.5 mmol HMF, 20 mL n-butanol, 0.1 g Fe-L1/C-800 catalyst, 1 MPa H_2 , $t=12$ h.

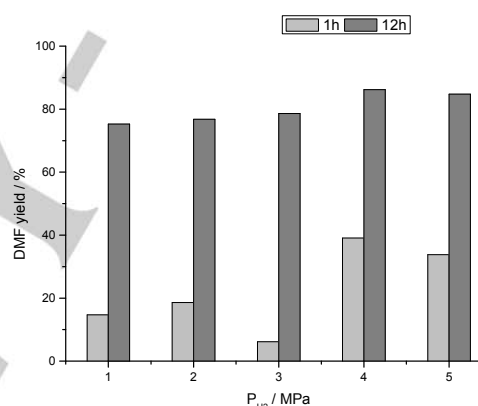


Figure 3. Effect of hydrogen pressure on the HDO of HMF to DMF. Reaction conditions: 0.5 mmol HMF, 20 mL n-butanol, 0.1 g Fe-L1/C-800 catalyst, $T=240$ °C, $t=1$ h or 12h.

DFF yield of 4.6%, indicating that the HDO of HMF was still inefficient. In addition, the HMF conversion was found to be much higher than the total yield of furanic compounds at these two reaction temperatures. This could be attributed to the generation of acetals or ethers byproducts from HMF confirmed by GCMS analysis. A significant enhancement in DMF yield was observed when the reaction temperature was further increased to 200 °C. However, some intermediates such as MF, MFM, and DHMF were still present in considerable quantities. The highest DMF yield of 75.3% was observed at 240 °C, and its yield was decreased slightly while the reaction temperature was further raised to 280 °C. In addition, acetals or ethers byproducts disappeared when the reaction temperature exceeded 240 °C. Thus, 240 °C was chosen as the optimal reaction temperature for further investigations.

Subsequently, as shown in figure 3, the effect of hydrogen pressure on the HDO of HMF to DMF was investigated at 240 °C with the Fe-L1/C-800 catalyst. At a reaction time of 1 h, the highest DMF yield of 39.1% was obtained at H₂ pressure of 4 MPa. In comparison, the DMF yield was only 6.2% at 3 MPa H₂. When the reaction was prolonged to 12 h, trace yields of intermediates such as MF and DHMF were observed at a hydrogen pressure of 1 MPa, and these products were undetectable at higher hydrogen pressures. In addition, no ring-hydrogenated products were observed even at a hydrogen pressure of 5 MPa. Full conversion of HMF was achieved in each case, and the highest DMF yield of 86.2% was observed at 4 MPa. Thus, a hydrogen pressure of 4 MPa was used in following experiments.

Effect of iron loading

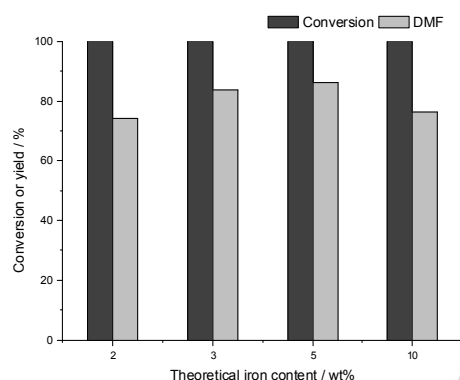


Figure 4. Effect of iron loading on the HDO of HMF to DMF. Reaction conditions: 0.5 mmol HMF, 20 mL n-butanol, 0.1 g Fe-L1/C-800 catalyst, 4 MPa H₂, t=12h.

Iron catalysts with four different iron contents were prepared to explore the effect of iron loading. The theoretical iron contents were determined as 2, 3, 5, 10 wt%, which were calculated by dividing the weight of iron in the iron precursors by the weight of carbon supports. However, the actual iron contents were 1.52, 2.19, 3.14, and 4.87 wt%, respectively. The differences could be attributed to the weight of the nitrogen precursors. In addition, the Fe/N molar ratios were 0.22, 0.26, 0.34, and 0.62, respectively. The catalyst dosage was kept constant during the examination. As shown in figure 4, full HMF conversion was observed in each catalytic experiment, and the highest DMF yield was achieved at a theoretical iron content of 5 wt%. Besides the target product DMF, only DFF was detected as the by-product at the lowest theoretical iron content of 2 wt% with a yield of 7.7%. Thus, it seems that a low iron loading would lead to an inefficient hydrogenation activity. The inferior catalytic performance of iron catalyst with 10 wt% loading suggested that higher Fe/N molar ratio would lead to lower DMF selectivity. Thus, the optimal iron loading was 5%.

Reaction Pathways

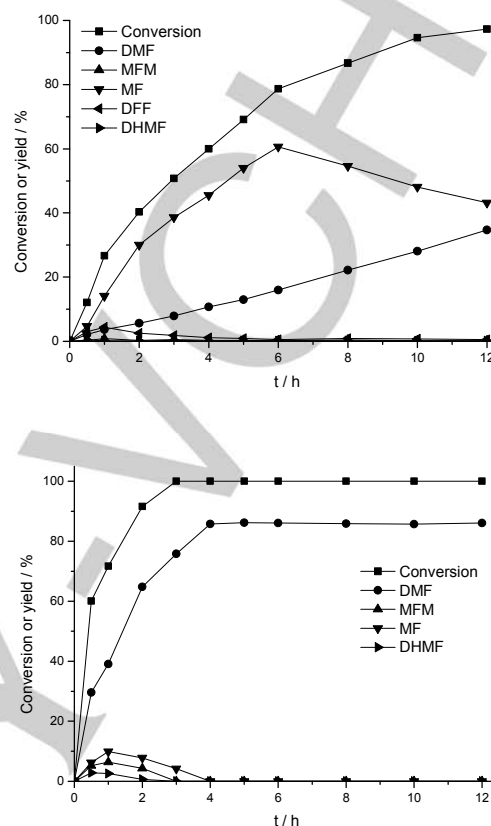


Figure 5. Product distributions of the HDO of HMF as a function of reaction time in THF (top) and n-butanol (bottom). Reaction conditions: 0.5 mmol HMF, 20 mL solvent, 0.1 g Fe-L1/C-800 catalyst, 4 MPa H₂.

On the basis of the above catalytic results, two preliminary key points could be summarized: (a) MF is a possible key intermediate in the catalytic reaction pathway; (b) DMF yield could be enhanced by using alcohols as both solvents and H-donors. In order to better understand the reaction pathways, we explored the product distribution of HMF HDO at different reaction time in THF and n-butanol (figure 5). While using THF as the solvent, the conversion of HMF increased gradually throughout the reaction time. In contrast, total conversion of HMF was achieved within 3 h with n-butanol as the solvent. Thus, the conversion rate of HMF was enhanced dramatically by promoting the hydrogen-donating ability of the solvent.

In addition, a significant difference in the intermediate product distribution in THF and n-butanol was also observed. When THF was used as the solvent, only 34.7% yield of the target product DMF was obtained at 12 h. MF was observed as the major by-product, which achieved a maximum yield of 60.6% at 6 h, and then decreased gradually. This product distribution demonstrated that the reaction rate of HMF HDO to MF was much higher than that of MF HDO to DMF, leading to the

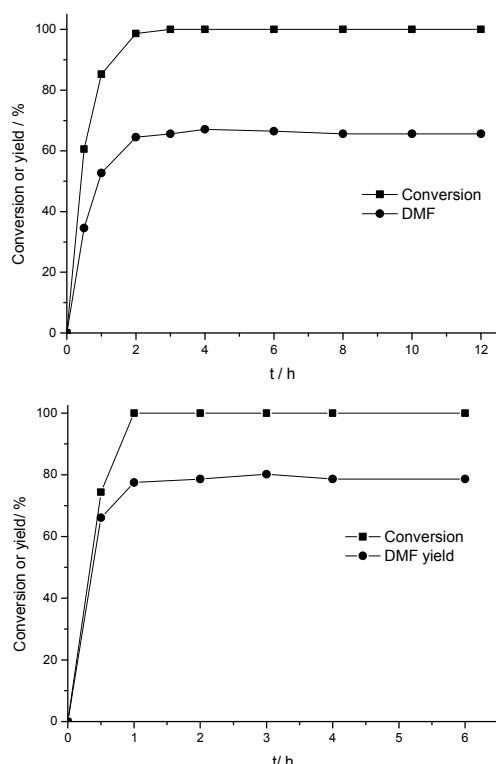


Figure 6. Product distributions of the HDO of MFM as a function of reaction time in THF (top) and n-butanol (bottom). Reaction conditions: 0.5 mmol MFM, 20 mL solvent, 0.1 g Fe-L1/C-800 catalyst, 4 MPa H₂.

accumulation of MF in the solution. Trace yields of other alcohol intermediates such as MFM and DHMF could be attributed to the high reaction rate of C-O bond HDO. When n-butanol was used as the solvent, the production rate of DMF was enhanced significantly, and a maximum yield of 86.2% was obtained within 5 h. MF achieved a maximum yield of 9.9% at 1 h, and then be converted completely after 6 h. In addition, DFF, which was the dehydrogenation product of HMF, achieved a maximum yield of 4.4% in THF, but could not be detected with n-butanol as the solvent. Thus, we proposed that promoting the hydrogen-donating ability of the solvent would significantly improve the reaction rate of the HDO of MF, thus leading to a higher yield and production rate of DMF.

We further carried out a series of experiments to demonstrate our hypothesis. In general, the HDO of MF could be divided into two reactions: (a) the hydrogenation of MF to MFM; (b) the HDO of MFM to DMF. We first explored the solvent effect on the HDO of MFM to DMF (figure 6). The complete conversion of MFM in THF was achieved within 2 h with a 65.6% yield of DMF. In comparison, slightly higher conversion rate of MFM and DMF yield were observed while using n-butanol as the solvent. Thus, it can be concluded that the hydrogen-donating ability of the solvent has considerable influence on the reaction rate of the

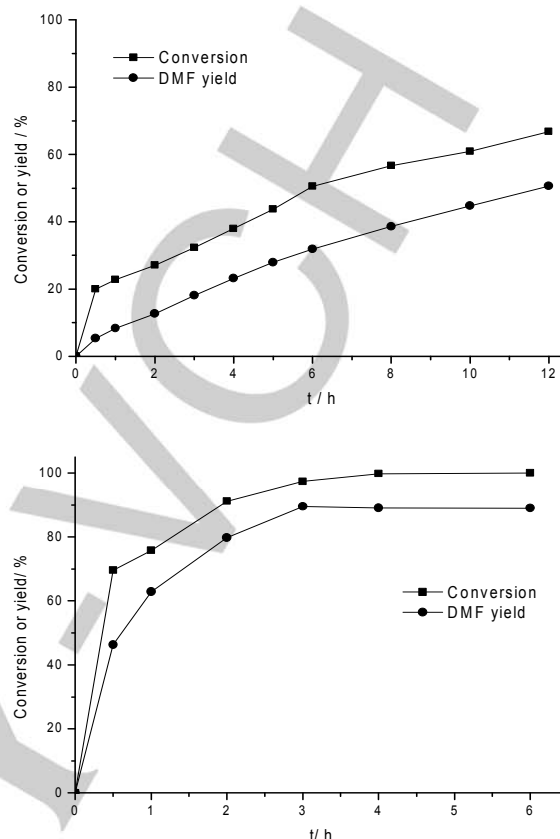


Figure 7. Product distributions of the HDO of MF as a function of reaction time in THF (top) and n-butanol (bottom). Reaction conditions: 0.5 mmol MF, 20 mL solvent, 0.1 g Fe-L1/C-800 catalyst, 4 MPa H₂.

HDO of C-O bond in MFM and the selectivity of target product DMF.

Subsequently, we explored the product distribution of MF HDO in THF and n-butanol (figure 7). It can be clearly seen that the HDO of MF proceeded fast in n-butanol, and a maximum DMF yield of 89.8% was observed at a reaction time of 2 h. In contrast, only 50.6% yield of DMF with a 66.8% conversion of MF was obtained in THF even though the reaction time was prolonged to 12 h. Thus, the HDO of MF was significantly accelerated by using solvent with stronger hydrogen donating-ability. This improvement was much more significant than that observed in the HDO of MFM to DMF. This enhancement could also be demonstrated by our latest work, in which the selective catalytic transfer hydrogenation of C=O bond in furfural was successfully achieved over this kind of heterogeneous iron catalysts with alcohols as the H-donors.^[42]

The HDO of MF and MFM over Fe/C-800 catalyst in n-butanol was explored to check the role of FeN_x species in the HDO of C=O and C-O bond (see figure S5 in the supporting information). The DMF yields were 44% and 53% for the HDO of MF and MFM, respectively. The inferior catalytic performance

Table 3. Catalytic HDO of various possible intermediates over Fe-L1/C-800 catalyst.^[a]

Entry	Solvent	Substrate	Conversion [%]	Yield [%]					CMB ^[b] [%]
				DMF	MF	MFM	DHMF	DFF	
1	THF	DHMF	100	63.1	8.7	-	-	-	71.8
2	THF	DFF	94.6	9.1	0.5	54.3	15.3	1.0	80.2
3	THF	DMF	<5%	-	-	-	-	-	-
4	n-butanol	DFF	96.3	85.2	-	-	-	-	85.2
5	n-butanol	DHMF	100	81.4	-	-	-	-	81.4
6	n-butanol	DMF	<5%	-	-	-	-	-	-

[a] Reaction conditions: 0.5 mmol substrate, 20 mL solvent, 0.1 g Fe-L1/C-800 catalyst, 4 MPa H₂, t=12h. [b] CMB is carbon mass balance, which is based on the detected known products.

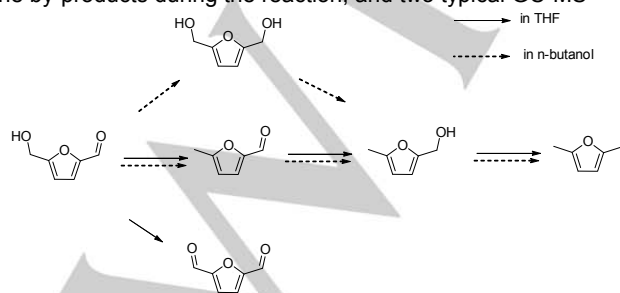
demonstrated that the presence of FeN_x species was critical to both HDO reactions.

We also conducted experiments with several other possible reaction intermediates such as DHMF, DFF, and product DMF (Table 3). The complete conversion of DHMF in THF was achieved with 63.1% yield of DMF and 8.7% yield of MF. The presence of MF demonstrated that the dehydrogenation of C-O bond occurred in THF. When n-butanol was used as the solvent, the DMF yield was increased to 81.4%, and no furanic by-products were detected. While we have demonstrated that the hydrogenation of C=O bond in MF was enhanced significantly by using n-butanol as the solvent, the hydrogenation of C=O bond in HMF was also possibly improved to form DHMF as the intermediate to produce DMF.

The catalytic results of DFF conversion further confirmed the difference between the HDO of C=O bond in THF and n-butanol. While using THF as the solvent, the major product was MF with a yield of 54.3%, and the yield of the target product DMF was only 9.1%. In addition, 15.3% yield of HMF was detected. In contrast, a 96.3% conversion of DFF with 85.2% DMF yield was observed by using n-butanol as the solvent. Thus, for the hydrogenation of C=O bond over heterogeneous iron catalysts, the catalytic transfer hydrogenation by H-donors was more preferable than direct hydrogenation by gaseous hydrogen.

The reactivity of product DMF in both solvents was also investigated. The conversion of DMF was lower than 5%, confirming the stability of DMF in the reaction condition.

Due to the unsatisfactory carbon balance (usually <90%) during the HMF conversion especially when using alcohols as the solvent, GC-MS analysis was performed to further identify the by-products during the reaction, and two typical GC-MS



Scheme 1. A plausible reaction pathway for the HDO of HMF to DMF over heterogeneous iron catalysts in THF and n-butanol.

spectra were shown in figure S2 (see the supporting information).

The overhydrogenation and ring-opening products of the furan ring in HMF were reported to be the major by-products in previous researches on the catalytic conversion of HMF to DMF over other transition metals with stronger hydrogenation ability. However, in this work, after checking all the experiments, including the time course during the reaction, we did not observe any overhydrogenation and ring-opening products in the GC-MS spectra. Thus, it was demonstrated that the iron catalysts did not destroy the aromatic structure in HMF during the HDO. Moreover, the only possible

HMF-derived by-product detected in GC-MS spectra was a dimer with a molecular weight of 190 (the recommended structure by NIST spectrum library is α -Furil) with a yield of ca. 4%, indicating that the polymerization of furanic compounds could be catalyzed by the Lewis acidity of the iron catalysts. Thus we proposed that the unsatisfactory carbon balance was probably due to the Lewis acid-catalyzed polymerization, leading to the formation of humins, which almost could not be detected in GC-MS. Hence, further effort will be devoted in the careful control of the hydrogenation ability and Lewis acidity of the iron catalysts to achieve higher DMF selectivity.

At last, on the basis of these experiments and previous researches, we proposed the following reaction pathway for the HDO of HMF to DMF over heterogeneous iron catalysts (scheme 1). When the reaction was performed in solvents with weak hydrogen-donating ability such as THF, the HDO of HMF to MF proceeded much faster than the HDO of MF to DMF, resulting in a large amount of MF in the product mixture with a low DMF yield. The hydrogenation of C=O bond was the rate-determine step during the reaction. In addition, the dehydrogenation of HMF to DFF also occurred. When solvents with higher hydrogen-donating ability were used, the hydrogenation of C=O bond was improved significantly by the catalytic transfer hydrogenation. Thus, both the hydrogenation of C=O bond and the HDO of C-O bond proceeded rapidly in alcohol solvents, and MF and DHMF were the possible intermediates during the reaction.

Recyclability

The recyclability of the heterogeneous iron catalysts was examined in five consecutive runs under identical reaction conditions, and the results were shown in figure 8. The used catalyst was recovered by centrifugation, washed with n-butanol for several times, and then used directly in next run. Complete conversions of HMF were achieved in each recycle run with similar DMF yields, and no other byproducts were observed. Thus, the catalytic activity of the iron catalyst maintained very well during the recycle test.

The excellent stability of the iron catalysts in the HDO of HMF was unexpected because this catalyst had represented an

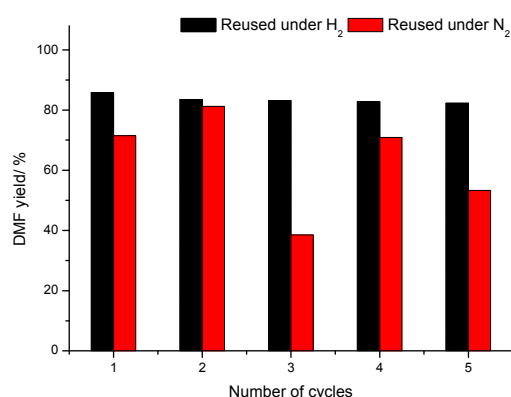


Figure 8. Recycling results of Fe-L1/C-800 for the HDO of HMF to DMF under two different reaction atmospheres. Reaction condition: 0.5 mmol substrate, 20 mL solvent, 0.1 g Fe-L1/C-800 catalyst, $t=12$ h, 4 MPa H₂ or 1 MPa N₂.

unsatisfactory stability in the catalytic transfer hydrogenation of furfural to furfuryl alcohol in our latest report. Accordingly, the destruction of N•••Fe species, the presence of crystallized Fe₂O₃ phase, and the pore structure change were the main reasons for the catalyst deactivation.^[52] The only difference between these two reactions is the reaction atmosphere. Thus, we proposed that the presence of hydrogen is essential to the maintenance of the catalytic activity. To test our hypothesis, the recyclability tests were then performed under an inert atmosphere. The yield of DMF increased slightly in the second run, and then dropped significantly in the third run. In addition, MF was detected as a byproduct with a yield of ca. 5% after the third cycle, suggesting a decrease in the hydrogenation ability of the iron catalyst after recycling under N₂. Although a considerable recovery of catalytic activity was observed in the fourth run, this catalyst was definitely unstable under the inert atmosphere.

To explore the reasons for the different stabilities of the iron catalysts under two different atmospheres, the reused catalysts were further characterized by XPS, XRD, and BET technologies.

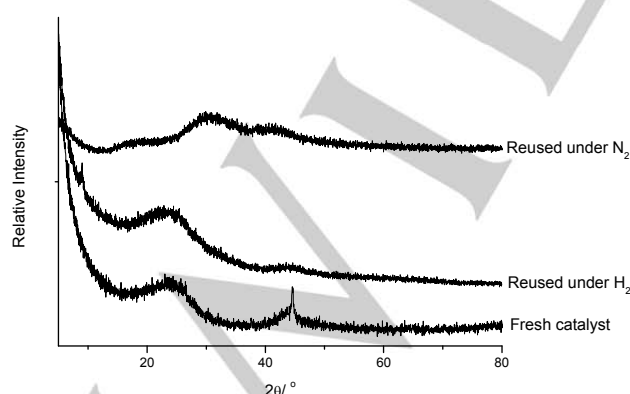


Figure 9. XRD patterns of fresh and reused Fe-L1/C-800 catalysts.

Table 4. Textural properties of the fresh and reused Fe-L1/C-800 catalysts.

Sample	BET surface area [m ² /g]	Pore Volume [cm ³ /g]	Pore Size [nm]
Fresh	830	0.89	4.27
Reused under H ₂	635	0.79	5.56
Reused under N ₂	495	0.53	5.03

The XPS spectrum of the Fe-L1/C-800 catalyst reused under H₂ clearly showed that the N•••Fe species was retained but with lower percentage content. In comparison, the peak of N•••Fe species slightly shifted to higher binding energies (from 399.7 eV to 399.9 eV) for the iron catalyst reused under N₂, and the percentage content of graphitic N increased dramatically, leading to the formation of a new peak at 401.3 eV in the XPS spectrum.

The XRD and BET characterization results also implicated that the structure of the iron catalyst was more easily destroyed under N₂ (figure 9). The peak of metallic iron at 44.6° in the XRD pattern of fresh Fe-L1/C-800 catalyst disappeared after recycling under H₂ for five runs. In comparison, significant changes in the XRD pattern were observed when the catalyst was reused under N₂, in which three broad humps at around 18°, 30°, and 41.5° were present. Some possible species such as amorphous carbon generally shows typical diffraction peaks of 26° and 43°, and Fe₂O₃ phase has a distinct peak at 35°. Thus, the peaks in the XRD pattern of catalyst reused under N₂ cannot be attributed to those species because of the considerable deviations. Nonetheless, the XRD patterns still suggested that the structure of the catalyst was destroyed more significantly when reused under N₂. The BET surface area and pore volume of Fe-L1/C-800 catalyst also decreased more dramatically while recycled under N₂ (Table 4), indicating that the porous structure of the catalyst was destroyed more significantly. In summary, the unexpected stability of the catalyst for the HDO of HMF could be attributed to the better reservation of the active species and the pore structure in the presence of H₂.

Continuous test

To further demonstrate the stability of the iron catalyst, the HDO of HMF was also performed in a continuous flow fixed-bed reactor in down-flow mode. The image and the diagram of the reactor could be seen in figure S7. The reactor system was consisted of a pump that introduced the liquid feed (25mM HMF n-butanol solution with toluene as the internal standard), into a stainless steel tubular reactor with an internal diameter of 17 mm and a length of 670 mm. The pressure over the system was controlled through a back-pressure regulator installed at the outlet of the reactor. The catalyst weight was 5.4 g (ca. 15 mL) and diluted with quartz sand (10 mL). The reaction was carried out at 240 °C with a LHSV of 0.4 h⁻¹. Owing to some limitations, the pressure was kept at only 0.7 MPa at a H₂ flow of 22 mL min⁻¹. The continuous test was performed for 72 h, and the results were shown in figure 10. To our delight, the catalysts did not deactivate after 72 h, suggesting its high stability during the

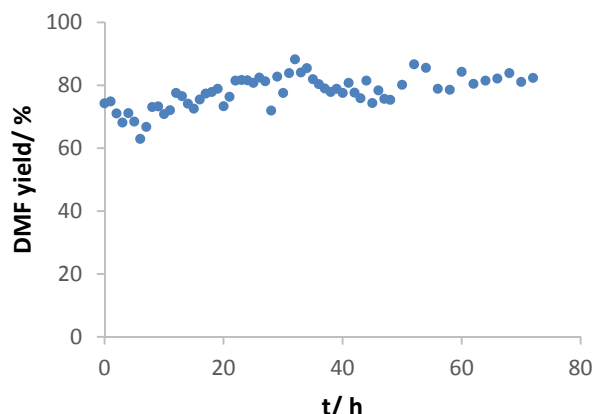


Figure 10. Dependence of DMF yield on time in the fixed-bed reactor. Reaction condition: 240 °C, 25mM HMF n-butanol solution mixed with toluene as the internal standard, LHSV=0.4 h⁻¹, p=0.7 MPa, H₂ flux=22 mL min⁻¹.

continuous test. The DMF yield was ca. 80%, which was slightly lower than the best results obtained in the batch reactor.

The catalyst after reaction was further characterized by XPS, XRD, and BET technologies. The XPS spectrum and the XRD pattern was similar to those of the fresh catalyst (figure S8). The new peak at 26.5° in the XRD pattern could be attributed to the quartz sand, which was hard to be isolated completely from the catalyst. The BET surface area was decreased to 630 m²/g, which was nearly the same as the catalyst reused under H₂ in the batch reactor (Table S2). To sum up, the iron catalyst was demonstrated to be stable during the continuous test in the presence of H₂.

Conclusions

The Iron-catalyzed HDO of HMF to DMF was explored in this work. The examination of the effect of the nitrogen precursor, support, pyrolysis temperature, and the metal center demonstrated that catalyst prepared by the pyrolysis of iron acetate and 1,10-phenanthroline on activated carbon at 800 °C was the most active heterogeneous iron catalyst. Complete conversion of HMF with an 86.2% selectivity of DMF was achieved in n-butanol at 240 °C for 5 h. Alcohol solvents could act as H-donors during the HDO, enhancing the reaction rate of the HDO reactions especially the hydrogenation of C=O bond. The excellent stability of the iron catalysts was demonstrated in batch and continuous flow fixed-bed reactors. The well reserved active species and the pore structure of the iron catalyst in the presence of H₂ was the key point. One of the main advantages of the iron catalyst system is that it did not hydrogenate the aromatic ring in HMF, which was beneficial to avoid the formation of overhydrogenation products and ring-opening products. However, the Lewis acidity of the iron catalyst will catalyze the polymerization of the furanic compounds to humins, causing a still unsatisfactory carbon balance during the reaction.

Thus, future work will focus on developing enhanced iron catalyst system with careful control of the hydrogenation ability and Lewis acidity to achieve higher DMF selectivity.

Experimental Section

List of chemicals

HMF, DHMF, and DFF were generous gifts from Hefei Leaf Energy Biotechnology Co., Ltd. DMF, MF, iron(II) acetate, 1,10-phenanthroline, 2,2'-bipyridine, 2,2':6',2''-terpyridine, hemin, and activated carbon were purchased from TCI. MFM was purchased from J&K Chemical. 8-hydroxyquinoline, phenylglycine, cobalt (II) acetate tetrahydrate, nickel acetate tetrahydrate, and alcohol solvents were purchased from Sinopharm Chemical Reagent Co. Ltd. Metal oxide supports such as titanium dioxide, silicon dioxide, and aluminium oxide were purchased from Aladdin Reagent Co. Ltd.

Catalyst preparation

The preparation of catalyst used a simultaneous pyrolysis of metal complex and carbon material similar to Beller et al.^[57] A typical procedure for catalyst preparation is described as follows: 0.5 mmol iron precursor and corresponding ligands were added to 50 mL ethanol under vigorously stirring at room temperature. Then 1 g activated carbon was added into the solution and the mixture was stirred at 60 °C for 15 h followed by rotary evaporation at 30 °C. Obtained solid was grinded into fine powder, and then pyrolyzed under an argon atmosphere with a gas flow rate of 100 mL/min in a tubular furnace.

Catalyst characterization

Transmission electron microscopy (TEM) was performed on a JEOL-2010 electron microscope. The samples were deposited on a Cu grids after ultrasonic dispersion of the samples in ethanol.

Nitrogen adsorption measurements were performed using an ASAP2020M adsorption analyzer which reports adsorption isotherm, specific surface area and pore volume automatically. The Brunauer-Emmett-Teller (BET) equation was used to calculate the surface area in the range of relative pressures between 0.05 and 0.20. The pore size was calculated from the adsorption branch of the isotherms using the thermodynamic 60 based Barrett-Joyner-Halenda (BJH) method.

XRD analysis was conducted on an X-ray diffractometer 65 (TTR-III, Rigaku Corp., Japan) using Cu K α radiation ($\lambda=1.54056$ Å). The data were recorded over 2 θ ranges of 10–70°.

XPS was obtained with an X-ray photoelectron spectroscopy (ESCALAB250, Thermo-VG Scientific, USA) using monochromatized Al K α radiation (1486.92 eV).

Temperature-programmed reduction (TPR) was conducted on a Quanta Chembet chemisorption instrument with a thermal conductivity detector (TCD). About 100 mg of samples was loaded in a quartz reactor, and then heated to 800 °C with a heating ramp rate of 10 °C min⁻¹ in a stream of 5% H₂/Ar with a total flow rate of 50 mL min⁻¹.

Experimental procedure

The catalytic HDO of HMF was carried out using a 50 mL Zr alloy autoclave provided by Anhui Kemi Machinery Technology Co., Ltd. For a typical procedure, 0.5 mmol HMF, 100 mg heterogeneous iron catalyst, and 20 mL solvent were added into the autoclave with a quartz lining. After purging the reactor with H₂, the reaction was conducted with 4 MPa

H₂ (room temperature) at 240 °C for 12 h with a stirring speed of 800 rpm. After reaction, the gaseous products were analyzed by using a Fuli 9790 II Gas Chromatograph with a thermal conductivity detector (TCD). The liquid products were analyzed by using both gas chromatography and Gas chromatograph-Mass spectrometry.

GC-MS analyses were performed on an Agilent 7890 Gas Chromatograph equipped with a DB-WAXETR 30 m × 0.25 mm × 0.25 µm capillary column (Agilent) or a HP-5MS 30 m × 0.25 mm × 0.25 µm capillary column (Agilent). The GC was directly interfaced to an Agilent 5977 mass selective detector (EI, 70 eV). The following GC oven temperature programs were used: 40 °C hold for 1 min, ramp 5 °C/min to a temperature of 120 °C, and then ramp 10 °C/min to 240 °C and hold for 5 min.

Acknowledgements

This work was supported by Science Foundation of China University of Petroleum, Beijing (No. 2462014YJRC037, C201604).

Keywords: biomass • heterogeneous catalysis • 5-hydroxymethylfurfural • hydrodeoxygenation • iron

- [1] G. W. Huber, S. Iborra, A. Corma, *Chem. Rev.* **2006**, *106*, 4044–4098.
- [2] A. Corma, S. Iborra, A. Velty, *Chem. Rev.* **2007**, *107*, 2411–2502.
- [3] R. J. van Putten, J. C. van der Waal, E. D. De Jong, C. B. Rasrendra, H. J. Heeres, J. G. de Vries, *Chem. Rev.* **2013**, *113*, 1499–1597.
- [4] R. L. Liu, J. Z. Chen, X. Huang, L. M. Chen, L. L. Ma, X. J. Li, *Green Chem.* **2013**, *15*, 2895–2903.
- [5] H. L. Wang, T. S. Deng, Y. X. Wang, Y. Q. Qi, X. L. Hou, Y. L. Zhu, *Bioresour. Technol.* **2013**, *136*, 394–400.
- [6] Y. Román-Leshkov, C. J. Barrett, Z. Y. Liu, J. A. Dumesic, *Nature*, **2007**, *447*, 982–985.
- [7] B. Girisuta, L. P. B. M. Janssen, H. J. Heeres, *Green Chem.* **2006**, *8*, 701–709.
- [8] F. Geilen, T. vom Stein, B. Engendahl, S. Winterle, M. A. Liauw, J. Klankermayer, W. Leitner, *Angew. Chem.* **2011**, *123*, 6963–6966; *Angew. Chem. Int. Ed.* **2011**, *50*, 6831–6834.
- [9] J. P. Ma, Z. T. Du, J. Xu, Q. H. Chu, Y. Pang, *ChemSusChem* **2011**, *4*, 51–54.
- [10] N. K. Gupta, S. Nishimura, A. Takagaki, K. Ebitani, *Green Chem.* **2011**, *13*, 824–827.
- [11] J. J. Pacheco, M. E. Davis, *Proc. Natl. Acad. Sci. USA* **2014**, *111*, 8363–8367.
- [12] T. Buntara, S. Noel, P. H. Phua, I. Melián-Cabrera, J. G. de Vries, H. J. Heeres, *Angew. Chem.* **2011**, *123*, 7221–7225; *Angew. Chem. Int. Ed.* **2011**, *50*, 7083–7087.
- [13] T. Thananathanachon, T. B. Rauchfuss, *Angew. Chem.* **2010**, *122*, 6766–6768; *Angew. Chem. Int. Ed.* **2010**, *49*, 6616–6618.
- [14] M. Chidambaram, A. T. Bell, *Green Chem.* **2010**, *12*, 1253–1262.
- [15] S. De, S. Dutta, B. Saha, *ChemSusChem* **2012**, *5*, 1826–1833.
- [16] J. Jae, W. Q. Zheng, R. F. Lobo, D. G. Vlachos, *ChemSusChem* **2013**, *6*, 1158–1162.
- [17] J. Jae, W. Q. Zheng, A. M. Karim, W. Guo, R. F. Lobo, D. G. Vlachos, *ChemCatChem* **2014**, *6*, 848–856.
- [18] D. Scholz, C. Aellig, I. Hermans, *ChemSusChem* **2014**, *7*, 268–275.
- [19] Y. H. Zu, P. P. Yang, J. J. Wang, X. H. Liu, J. W. Ren, G. Z. Lu, Y. Q. Wang, *Appl. Catal. B* **2014**, *146*, 244–248.
- [20] L. Hu, X. Tang, J. X. Xu, Z. Wu, L. Lin, S. J. Liu, *Ind. Eng. Chem. Res.* **2014**, *53*, 3056–3064.
- [21] M. Chatterjee, T. Ishizaka, H. Kawanami, *Green Chem.* **2014**, *16*, 1543–1551.
- [22] A. S. Nagpure, N. Lucas, S. V. Chilukuri, *ACS Sustainable Chem. Eng.* **2015**, *3*, 2909–2916.
- [23] A. S. Nagpure, A. K. Venugopal, N. Lucas, M. Manikandan, R. Thirumalaiswamy, S. Chilukuri, *Catal. Sci. Technol.* **2015**, *5*, 1463–1472.
- [24] J. Luo, L. Arroyo-Ramírez, R. J. Gorte, *AIChE J.* **2015**, *61*, 590–597.
- [25] J. J. Shi, Y. Y. Wang, X. N. Yu, W. C. Du, Z. Y. Hou, *Fuel* **2016**, *163*, 74–79.
- [26] A. B. Gawade, M. S. Tiwari, G. D. Yadav, *ACS Sustainable Chem. Eng.* **2016**, *4*, 4113–4123.
- [27] G. H. Wang, J. Hilgert, F. H. Richter, F. Wang, H. Bongard, B. Spliethoff, C. Weidenthaler, F. Schüth, *Nature Mater.* **2014**, *13*, 293–300.
- [28] J. Luo, H. Yun, A. V. Mironenko, K. Goulas, J. D. Lee, M. Monai, C. Wang, V. Vórotnikov, C. B. Murray, D. G. Vlachos, P. Fornasiero, R. J. Gorte, *ACS Catal.* **2016**, *6*, 4095–4104.
- [29] J. Luo, J. D. Lee, H. Yun, C. Wang, M. Monai, C. B. Murray, P. Fornasiero, R. J. Gorte, *Appl. Catal. B* **2016**, *199*, 439–446.
- [30] J. M. R. Gallo, D. M. Alonso, M. A. Mellmer, J. A. Dumesic, *Green Chem.* **2013**, *15*, 85–90.
- [31] B. Saha, C. M. Bohn, M. M. Abu-Omar, *ChemSusChem*, **2014**, *7*, 3095–3101.
- [32] S. Nishimura, N. Ikeda, K. Ebitani, *Catal. Today*, **2014**, *232*, 89–98.
- [33] J. Luo, L. Arroyo-Ramírez, J. F. Wei, H. Yun, C. B. Murray, R. J. Gorte, *Appl. Catal. A* **2015**, *508*, 86–93.
- [34] T. S. Hansen, K. Barta, P. T. Anastas, P. C. Ford, A. Riisager, *Green Chem.* **2012**, *14*, 2457–2461.
- [35] A. J. Kumalaputri, G. Bottari, P. M. Erne, H. J. Heeres, K. Barta, *ChemSusChem* **2014**, *7*, 2266–2275.
- [36] G. Bottari, A. J. Kumalaputri, K. K. Krawczyk, B. L. Feringa, H. J. Heeres, K. Barta, *ChemSusChem* **2015**, *8*, 1323–1327.
- [37] Y. B. Huang, M. Y. Chen, L. Yan, Q. X. Guo, Y. Fu, *ChemSusChem* **2014**, *7*, 1068–1070.
- [38] M. Y. Chen, C. B. Chen, B. Zada, Y. Fu, *Green Chem.* **2016**, *18*, 3858–3866.
- [39] X. Kong, Y. F. Zhu, H. Y. Zheng, F. Dong, Y. L. Zhu, Y. W. Li, *RSC Adv.* **2014**, *4*, 60467–60472.
- [40] X. Kong, Y. F. Zhu, H. Y. Zheng, X. Q. Li, Y. L. Zhu, Y. W. Li, *ACS Catal.* **2015**, *5*, 5914–5920.
- [41] X. Kong, R. X. Zheng, Y. F. Zhu, G. Q. Ding, Y. L. Zhu, Y. W. Li, *Green Chem.* **2015**, *17*, 2504–2514.
- [42] Y. F. Zhu, X. Kong, H. Y. Zheng, G. Q. Ding, Y. L. Zhu, Y. W. Li, *Catal. Sci. Technol.* **2015**, *5*, 4208–4217.
- [43] X. M. Xiang, J. L. Cui, G. Q. Ding, H. Y. Zheng, Y. L. Zhu, Y. W. Li, *ACS Sustainable Chem. Eng.* **2016**, *4*, 4506–4510.
- [44] P. P. Yang, Q. N. Xia, X. H. Liu, Y. Q. Wang, *Fuel* **2017**, *187*, 159–166.
- [45] B. F. Chen, F. B. Li, Z. J. Huang, G. Q. Yuan, *Appl. Catal. B* **2017**, *200*, 192–199.
- [46] L. L. Yu, L. He, J. Chen, J. W. Zheng, L. M. Ye, H. Q. Lin, Y. Z. Yuan, *ChemCatChem* **2015**, *7*, 1701–1707.
- [47] M. Lefèvre, E. Proietti, F. Jaouen, J. P. Dodelet, *Science*, **2009**, *324*, 71–74.
- [48] G. Wu, K. L. More, C. M. Johnston, P. Zelenay, *Science*, **2011**, *332*, 443–447.
- [49] R. V. Jagadeesh, A. E. Surkus, H. Junge, M. M. Pohl, J. Radnik, J. Rabeah, M. Beller, *Science*, **2013**, *342*, 1073–1076.
- [50] R. V. Jagadeesh, H. Junge, M. Beller, *ChemSusChem* **2015**, *8*, 92–96.
- [51] T. Stemmler, A. Surkus, M. Pohl, K. Junge, M. Beller, *ChemSusChem* **2014**, *7*, 3012–3016.
- [52] J. Li, J. L. Liu, H. J. Zhou, Y. Fu, *ChemSusChem* **2016**, *9*, 1339–1347.
- [53] S. Sitthitha, W. An, D. E. Resasco, *J. Catal.* **2011**, *284*, 90–101.
- [53] R. A. Rajadhyaksha, S. L. Karwa, *Chem. Eng. Sci.* **1986**, *41*, 1765–1770.
- [54] R. V. Jagadeesh, H. Junge, M. Beller, *Nat. Commun.* **2014**, *5*, 4123.

- [55] X. J. Cui, Y. H. Li, S. Bachmann, M. Scalone, A. Surkus, K. Junge, C. Topf, M. Beller, *J. Am. Chem. Soc.* **2015**, *137*, 10652–10658.
- [56] R. A. Rajadhyaksha, S. L. Karwa, *Chem. Eng. Sci.* **1986**, *41*, 1765–1770.
- [57] R. V. Jagadeesh, T. Stemmler, A. E. Surkus, H. Junge, K. Junge, M. Beller, *Nat. Protoc.* **2015**, *10*, 548–557.

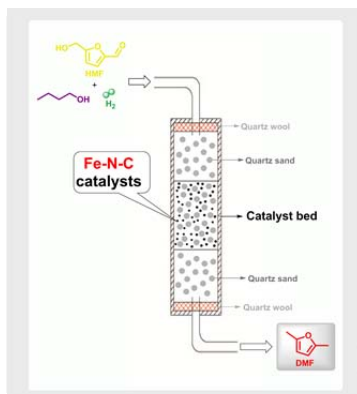
WILEY-VCH

Accepted Manuscript

Entry for the Table of Contents

FULL PAPER

Selective catalytic hydrodeoxygenation of 5-hydroxymethylfurfural to 2,5-dimethylfuran over heterogeneous iron catalysts is demonstrated in batch and continuous flow fixed-bed reactors. The iron catalyst exhibited excellent stability, which is probably due to the well reserved active species and the pore structure of the iron catalyst in the presence of H_2 .



Jiang Li,* Jun-ling Liu, He-yang Liu, Guang-yue Xu, Jun-jie Zhang, Jia-xing Liu, Guang-lin Zhou, Qin Li, Zhi-hao Xu, and Yao Fu*

Page No. – Page No.

Selective Hydrodeoxygenation of 5-Hydroxymethylfurfural to 2,5-Dimethylfuran over Heterogeneous Iron Catalysts